MASS TRANSFER PROPERTIES (PERMEABILITY AND MASS DIFFUSIVITY) OF FOUR AUSTRALIAN HARDWOOD SPECIES

Adam L. Redman,[a,b,*] Henri Bailleres,[b] Ian Turner,[a] and Patrick Perré [c]

Characterization of mass transfer properties was achieved in the longitudinal, radial, and tangential directions for four Australian hardwood species: spotted gum, blackbutt, jarrah, and messmate. Measurement of mass transfer properties for these species was necessary to complement current vacuum drying modeling research. Water-vapour diffusivity was determined in steady state using a specific vapometer. Permeability was determined using a specialized device developed to measure over a wide range of permeability values. Permeability values of some species and material directions were extremely low and undetectable by the mass flow meter device. Hence, a custom system based on volume evolution was conceived to determine very low, previously unpublished, wood permeability values. Mass diffusivity and permeability were lowest for spotted gum and highest for messmate. Except for messmate in the radial direction, the four species measured were less permeable in all directions than the lowest published figures, demonstrating the high impermeability of Australian hardwoods and partly accounting for their relatively slow drying rates. Permeability, water-vapour diffusivity, and associated anisotropic ratio data obtained for messmate were extreme or did not follow typical trends and is consequently the most difficult of the four woods to dry in terms of collapse and checking degradation.

Keywords: Water-vapour diffusivity; Permeability; Mass transfer; Hardwood; Anisotropy

*Contact information: a: Mathematical Sciences, Faculty of Science and Technology, Queensland University of Technology, 2 George Street, GPO Box 2434, Brisbane, Queensland, 4001, Australia; b: Agri-Science Queensland, Department of Employment, Economic Development and Innovation, Queensland Government. 50 Evans Road, Salisbury, Queensland, Australia; c: École Centrale Paris, LGPM, Grande Voie des Vignes, 92290 Châtenay-Malabry, France; *Corresponding author: adam.redman@deedi.qld.gov.au*

INTRODUCTION

In recent years, with emerging technological advancements in construction, design, computer control, and less expensive materials, vacuum drying of hardwood timber, particularly in Europe and USA, has proven in many applications to be a more economic alternative to drying using conventional methods, with similar or better quality outcomes (2004). In light of this, the Australian hardwood timber industry invested in a project with Queensland Government's Department of Employment, Economic Development and Innovation (DEEDI) to establish the viability of vacuum drying technology for the drying of four high volume and value commercial Australian hardwood species with respect to drying quality, time, and cost. Australian *Eucalyptus* are notoriously difficult to dry without degradation (Vermaas 1995; Vermaas and Bariska

1995). Moreover, it was recognized that a better knowledge of the material and associated drying behavior is required to fully optimize the vacuum drying process in the future. Therefore, a component to develop a hardwood vacuum drying model was included in the project.

Currently, much modeling work has been conducted for softwood species due to its commercial importance and relative homogeneity between species (Pang 2007; Perré *et al*. 2007; Perré and Turner 1999a; Salin 1991; Turner and Perré 1995). The complexity of the wood structure of hardwoods, paired with the huge variation within and between species has resulted in limited deterministic modeling work being performed to date on these species.

Previous research (Perré and Passard 2004; Salin 2010) has identified a number of essential wood properties that must be measured to provide the necessary structure for developing an accurate drying model. For the mass transfer component of drying modeling, measurement of the key parameters permeability and water-vapour diffusivity are required. Knowledge of these parameters is also important for understanding and describing the mechanisms that govern wood preservative impregnation. Very little data is available on the permeability and water-vapour diffusivity characteristics for the species under investigation.

The objectives of this study were to characterize (1) the air permeability, which defines the mass flux in response to a pressure gradient, and (2) the water-vapour diffusivity, which defines the mass flux in response to a concentration gradient, of four highly commercial Australian hardwood species to complement current vacuum drying modeling research. This research takes advantage of the existing deterministic model *TransPore* (Perré and Turner 1999a,b) used to predict the drying behavior of softwoods and drying of other porous media such as concrete.

The species under investigation are mature native forest spotted gum (*Corymbia citriodora* Hook), blackbutt (*Eucalyptus pilularis* Sm), jarrah (*Eucalyptus marginata* D.Don ex Sm.), and messmate (*Eucalyptus obliqua* L'Herit.). The species were chosen based on their large commercial volume, value, and range of drying characteristics and wood properties. For example, spotted gum is the easiest species to dry in terms of resistance to drying degrade and has the highest basic density (BD) of 1000 kg/m^3 (Bootle 2004), followed by blackbutt (710 kg/m^3 BD) and jarrah (670 kg/m^3 BD), which are mildly susceptible to surface checking. Finally, messmate is one of Australia's hardest species to dry due to its propensity to collapse and internal and surface check, and because it has the lowest BD of 630 kg/m^3. This raises the question as to what role do wood anatomy and properties play in the vastly different drying behaviors of these species. This forms the basis of the study.

EXPERIMENTAL

Materials

Material for this study was selected from kiln dried material from concurrent vacuum drying studies (Redman 2011), where the median density board most closely aligned to the average drying rate during a drying trial. Thus, for each species, the board

having the median basic density was selected from a quantity of 100 samples to measure the mass transfer properties. For each species, one quartersawn and one backsawn board with dimensions 300 x 100 x 8 mm (L, R, T and L, T, R orientations, respectively) were prepared. Three 74 mm diameter samples were cut using an 80 mm diameter hole-saw for each board producing three radial and three tangential (in thickness direction) samples per species. Also, one 200 x 100 x 28 mm thick sample was prepared. From those boards, three 19 mm diameter, 20 mm long cylinders were cut using a 24 mm hole-saw in the same longitudinal symmetry plane (Fig. 1). These samples were used to determine longitudinal permeability. Due to the amazingly low permeability encountered for spotted gum, the samples were cross cut in half to produce 10 mm long samples. The side surfaces of all specimens were coated with two layers of epoxy resin to guarantee the air tightness of the lateral surfaces during measurement.

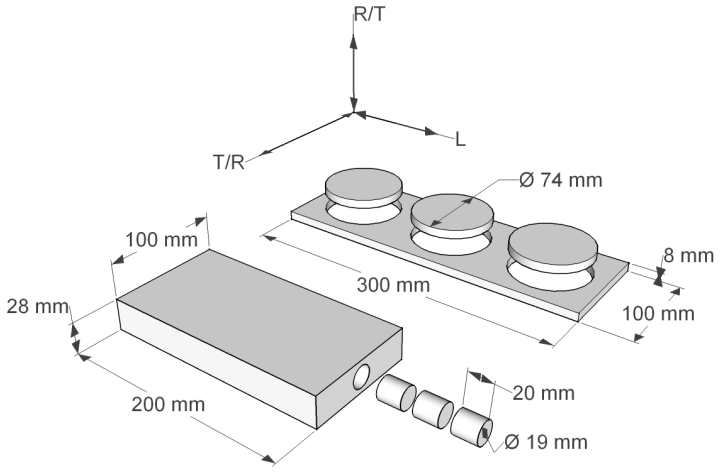

Fig. 1. Sample preparation for permeability tests: foreground – longitudinal (L) sampling, background – radial (R), and tangential (T) sampling

Methods

Permeability

The need to carry out measurements of permeability to air of various species, along the three material directions and at different pressure levels requires an accurate and reliable device capable of measurement over a wide range of permeability values. For this purpose, the team at AgroParisTech, France developed a system called ALU-CHA as described by Rousset *et al.* (2004).

The originality of this medium lies in a high reliability of lateral air tightness, the rapid operation, and the possibility to measure permeability with the same samples as those employed for the diffusion measurements. This device (Fig. 2) allows us to apply an accurate and constant pressure difference between the two faces of the sample. We can determine the corresponding gas flux by a mass flow meter, whose principle lies in the measurement of the thermal perturbation due to the gas flux when it passes through a capillary tube.

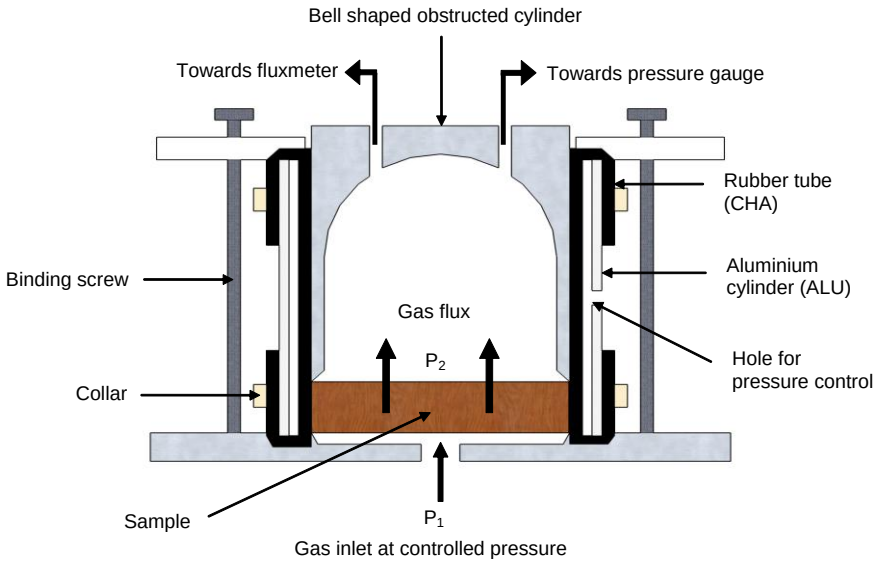

Fig. 2. Schematic of sample support with ALU-CHA system for permeability measurements

Note the presence of a rubber tube around the sample. A partial vacuum is applied over the hole in the aluminum chamber, sucking the rubber tube to the aluminum chamber to easily place or remove the sample. Then, during measurement, a typical pressure of 2 to 3 bar is applied in this chamber to press the rubber joint against the lateral face of the sample for air tightness. In addition, before placing the specimen in the ALU-CHA system, a silicone-based grease of high viscosity (vacuum grease) was applied on the lateral surfaces of the specimen to inhibit surface flow in the micro-porosity layer formed between the epoxy resin and rubber surfaces. The measurement was carried out by applying a controlled and constant pressure difference (ΔP) between two faces of the specimen and then measuring the corresponding air flux (Q). All measurements were performed in a temperature-controlled room with minimum temperature fluctuations. Due to the effect of temperature on the air viscosity, the room temperature was also recorded for each measurement. The air flux permeating through the specimen was recorded when the flow meter exhibited a nearly constant airflow. The air permeability of each sample was then calculated by Darcy's law (Dullien 1992),

$$K = \frac{Q\mu eP}{A\Delta P\overline{P}} \quad (1)$$

where K is the intrinsic permeability (m^2); Q is the air flux ($m^2\ s^{-1}$); μ is the dynamic viscosity of air (Pa s); e is the sample thickness (m); P is the pressure at which flux Q is measured (Pa); A is the sample area (m^2); $\Delta P = P_2 - P_1$ is the pressure difference between the air outlet (P_2) and inlet (P_1) sides of the sample (Pa); $\overline{P} = (P_1+P_2)/2$ is the averaged pressure inside the sample (Pa).

For each measurement, three pressure differentials were tested between 100 and 1000 mbar. The validity of Darcy's law was demonstrated for all test samples by the linear correlation found between the pressure difference (ΔP) and air flux (Q).

We remark that although Knudsen diffusion for gas flow was considered as a potential factor affecting the accuracy of permeability measurements, it was assumed negligible for the gas permeability measurements performed here. To justify this, we argue as follows: It is well known that when the capillary dimensions are smaller or of the same order as the mean free path (the average distance molecules travel between collisions), Knudsen diffusion or slip flow occurs because the molecules frequently collide with the capillary wall. The mean free path of air molecules at 20°C and 1 atmosphere is 0.068 µm, and slip flow is significant in capillary openings near this size or smaller (Siau 1984). However, as the average pit aperture diameter for eucalypts is reported to be 0.6 µm (Moura and Figuerido 2002), a factor of 10 times larger than the mean free path, the effect of Knudsen diffusion or slip flow on gas permeability measurements was deemed negligible.

Two ALU-CHA systems were used to cater for the two diameter classes of specimens. One system was used for the longitudinal samples and another for the larger diameter transverse samples.

For most species, permeability measurements in the radial and tangential directions could not be achieved using the regular experimental set-up, as the permeability was too low (less than 10^{-18} m^2), which is below the range offered by the flow meter. Consequently, the flow meter was disconnected and a custom system, based on volume evolution, was conceived and subsequently connected to the gas output of the ALU-CHA system. This entailed a flexible silicon hose connected to a glass tube with an internal radius of 2.87 mm. The radius of the tube was calibrated using a laboratory pipette. The glass tube was placed in a beaker of water next to a 0.5 mm increment gauge (Fig. 3). The permeability of the sample could then be measured using Equation 1, where the flux was determined by measuring the volume of the displacement of water in the tube as a function of time (measured using a chronometer) at different pressure gaps. Instead of measuring permeability over a matter of seconds or minutes, the flow was so low that, in spite of the small tube diameter, hours or days were required to obtain accurate measurements using this method. This method, although relatively simple, was able to increase the range of permeability values by 4 orders of magnitude, from 10^{-18} to 10^{-22} m^2.

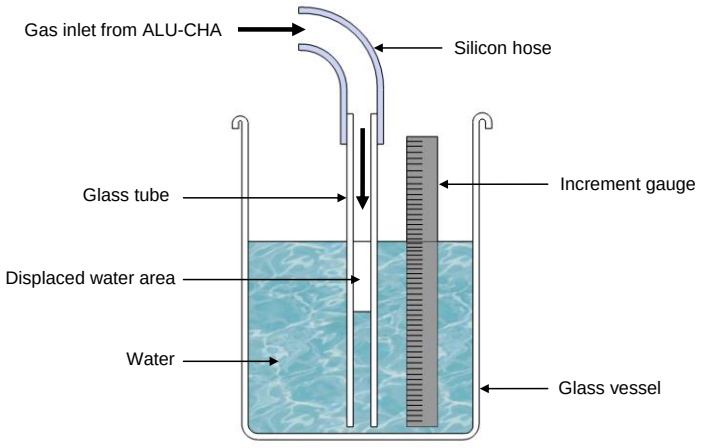

Fig. 3. Schematic of system developed to measure samples with very low permeability

The effect on the back pressure caused by the water in the glass during testing was not included in the calculations, as it was thought to be insignificant. As the height of displaced water measured was never more than 10 mm, this represents a static back pressure of approximately 1 mbar. When compared to the pressure gap imposed on both sides of the sample ranging from 100 to 1000 mbar, the effect of the water column represents an error 1 to 0.1%, respectively.

Water-vapour diffusivity

The same specimens were used to determine the mass diffusion coefficient as those used to measure permeability in each direction for each species.

Due to its reduced complexity, the steady-state determination of water-vapour diffusivity was chosen, whereby two different values of air humidity are applied on each side of the sample. The principle of measurement in the steady-state regime uses the technique of the vaporimeter (Fig. 4). The vaporimeters used for these experiments are based on the PVC-CHA system developed by the team at AgroParisTech, France as described by Agoua and Zohoun (2001).

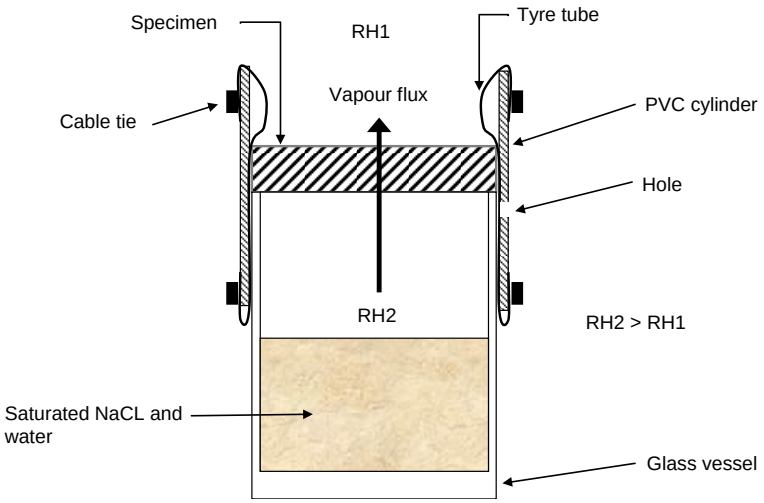

Fig. 4. Schematic of sample support with PVC-CHA system for water-vapour diffusivity measurements

Wood specimens were initially equalized in a constant humidity and temperature chamber at 75 ± 2% relative humidity and 35 ± 0.1ºC to produce equilibrium conditions of 14% moisture content (MC).

The circular specimens were placed onto similar diameter cylindrical glass vessels containing a saturated solution of de-ionized/purified water and chemical grade (>99.9%) NaCl. For a given temperature, the partial pressure of vapor relates directly to relative humidity. A saturated salt solution inside the vessel generates a relative humidity (RH2) of 75% at 35ºC.

To create an airtight seal around the device, a cylinder of PVC was used with an attached piece of inner tube inside the PVC clamped using cable ties. A small hole was drilled into the side of the PVC pipe. Using a vacuum, air was aspirated through the hole,

thus sucking the inner tube against the PVC pipe. This enabled the apparatus to be lowered over the specimen and glass. By releasing the vacuum, the inner tube relaxes tightly against the specimen and the vessel, creating an airtight seal.

The vaporimeter devices were placed into the constant environment chamber at 35ºC and 40% relative humidity (RH1) to produce equilibrium conditions of 7% MC. With this device assembly, two different relative humidity levels occur on each side of the wood specimen to create a diffusive flux driving force through the sample. The device was used to measure the vapor flux by weighing the device periodically over time and measuring the overall weight loss. The samples were weighed inside the constant environment chamber via sealed glove gauntlets in the chamber door, and a mass balance, accurate to 1 mg, placed inside the chamber. This allows mass flux measurements without disruption of conditions of temperature and humidity, and assures their good stability whatever the duration of testing.

By plotting the weight change as a function of time, a steady-state relationship is observed after a few days when the plot becomes a straight line (linear relationship between weight change and time). The diffusion coefficient through gross wood (D_b) is then calculated from the following formula (Siau 1984),

$$D_b = \frac{mL}{tAG\rho_w \Delta X} \quad (2)$$

where m is the mass of vapor transferred (kg); L is the specimen thickness (m); t is time (s), A is the specimen surface area (m^2); G is the specific gravity of the specimen at moisture content X; ρ_w is the density of water (kg m^{-3}); and ΔX is the moisture content difference between the two parallel surfaces of the specimen (kg kg^{-1}). ΔX is calculated using,

$$\Delta X = \frac{X_b + X_t}{2}, \quad (3)$$

where Xb is the moisture content of the specimen bottom (kg kg^{-1}); X_t is the moisture content of the specimen top (kg kg^{-1}). For these tests, Xb and X_t were calculated using previously determined specific sorption/desorption isotherms for each species (Redman 2011).

RESULTS AND DISCUSSION

Permeability

The average permeability results measured for each species in the longitudinal, radial, and tangential directions are given in Table 1. The results highlight the dramatic anisotropy ratios of these species and the vast difference between species. It is stated in Perré (2007) that "wood has dramatic anisotropy ratios: the longitudinal permeability can be 1000 times greater than the transverse permeability for softwoods, and more than 10^6

for hardwoods". This is certainly the case for the species measured here, where the longitudinal to transverse anisotropy ratio was in the order of 10^6 for some species. No permeability values were measured for spotted gum in the radial direction as, even after 24 hours, no noticeable measurement could be made, indicating this species is highly impermeable in this direction ($<10^{-23}$ m^2).

Table 1. Longitudinal (L), Radial (R), and Tangential (T) Permeability (K) and Anisotropy Ratios for Spotted Gum, Blackbutt, Jarrah, and Messmate

Species	K (m^2)			Anisotropy Ratio		
	L×10^{-15}	R×10^{-18}	T×10^{-18}	K_L/K_R	K_L/K_T	K_R/K_T
Spotted gum	0.4	-	0.003		4750	
Blackbutt	35.0	0.01	0.02	2440000	2305000	0.9
Jarrah	67.4	0.05	0.04	3005000	1531000	1.1
Messmate	55.5	8.6	0.30	16400	3086000	177

Spotted gum was the least permeable species, with the permeability order of magnitude of the other species changing depending on wood direction. The radial to tangential permeability anisotropy ratio of messmate was in the order of 10^2 and is markedly higher than the other species tested. Table 2 shows permeability for other species published by Agoua and Perré (2010). Data are provided for maritime pine and spruce (softwoods), beech (temperate hardwood), and teak (tropical hardwood). Except for messmate in the radial direction, the four species measured in this work were less permeable in all directions than the lowest published figure shown in Table 2. This demonstrates the high impermeability of Australian hardwoods compared to other species reported (Agoua and Perré 2010) partly accounting for their relatively slow drying rates.

Table 2. Published Longitudinal (L), Radial (R), and Tangential (T) Gas Permeability (K) and Anisotropy Ratios for Other Species (Agoua and Perré 2010)

	K (m^2)			Anisotropy Ratio		
Species	L×10^{-15}	R×10^{-18}	T×10^{-18}	K_L/K_R	K_L/K_T	K_R/K_T
Maritime pine *(Pinus pinaster)*	328	1650	542	199	606	3
Spruce (*Picea abies*)	94	110	516	858	182	0.2
Beech (*Fagus sylvatica*)	742	74	367	9970	2020	0.2
Teak (*Tectona grandis*)	1750	4.82	5.69	363000	307000	0.8

Water-Vapour Diffusivity

Figures 5 through 8 show the evolution of mass loss over time in the transverse and longitudinal directions for each species. As radial and tangential sample diameters were much larger than those in the longitudinal direction, and because the samples were of slight varying thickness, to correct for the effect of sample geometry, the mass loss

was divided by the sample cross-sectional area and multiplied by the sample length. Both figures show two distinctive groups of curves, one of small slopes and one of extensive, larger slopes. The large sloped curves represent fluxes of water vapor in the longitudinal direction, and the small sloped curves through the transverse directions.

The vapor flux in all directions is markedly lower for spotted gum than for messmate, with the other species falling in between. This may be attributed to the vast anatomical and chemical differences between these species (Redman *et al*. 2011) that would lead to different structural parameters (Agoua and Perré 2010).

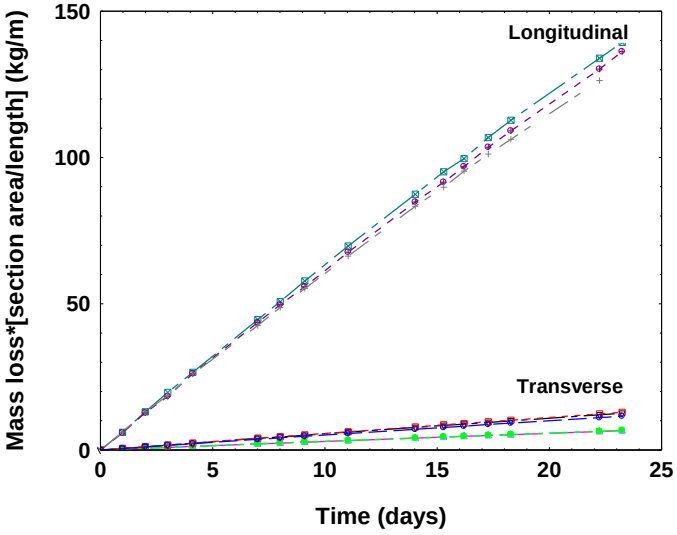

Fig. 5. Evolution of bound water flux corrected for sample geometry in the R, T, and L directions for messmate

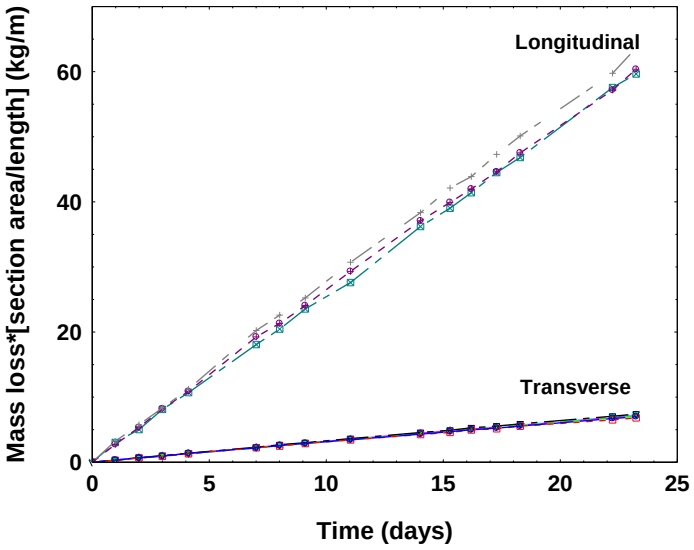

Fig. 6. Evolution of bound water flux corrected for sample geometry in the R, T, and L directions for jarrah

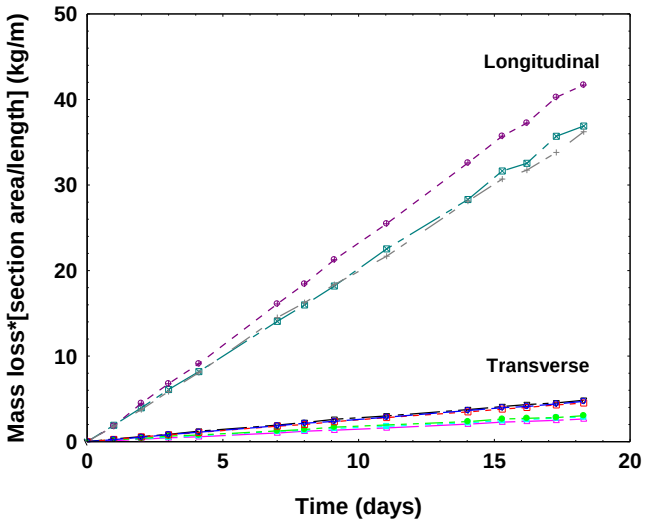

Fig. 7. Evolution of bound water flux corrected for sample geometry in the R, T, and L directions for blackbutt

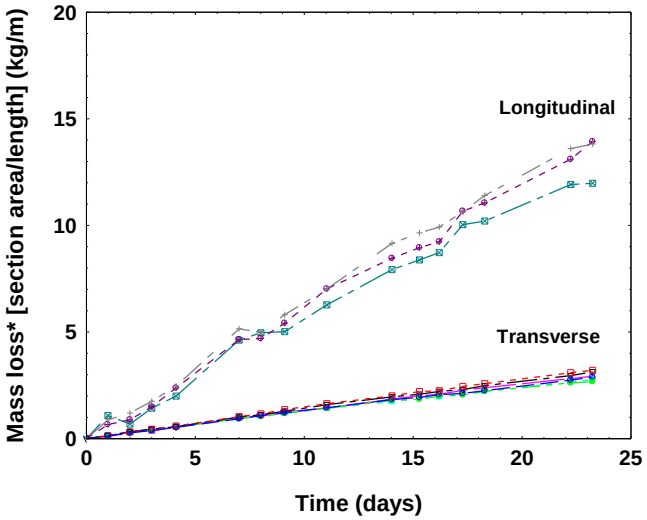

Fig. 8. Evolution of bound water flux corrected for sample geometry in the R, T, and L directions for spotted gum

Table 3 contains the measured diffusion coefficients in the radial, tangential, and longitudinal directions for each species. Spotted gum diffusion coefficients were much lower in all directions compared with the other species tested, with messmate having the highest value. The radial to tangential anisotropic ratio of the diffusion coefficient for spotted gum was approximately 1:1, indicating a behavior close to isotropy in this plane. This is evident in many other wood property ratios measured for this species (Redman *et al*. 2011). The converse is true for the other species tested, where relatively higher diffusion coefficient anisotropy ratios were observed, which is again reflective of the other wood properties measured for these species.

Table 3. Longitudinal (L), Radial (R), and Tangential (T) Diffusion Coefficients (D_b) and Anisotropy Ratios for Spotted Gum, Blackbutt, Jarrah, and Messmate.

Sample #	D_b (m^2 s^{-1})			Anisotropy ratio		
	L×10^{-10}	R×10^{-10}	T×10^{-10}	D_{bL}/D_{bR}	D_{bL}/D_{bT}	D_{bR}/D_{bT}
Spotted gum	0.6	0.1	0.1	4.2	4.2	1.0
Blackbutt	2.3	0.3	0.2	8.8	14.2	1.6
Jarrah	2.7	0.3	0.4	10.5	7.2	0.7
Messmate	10.3	0.7	0.4	14.6	25.4	1.7

Published diffusion coefficient data measured using the steady-state method is shown in Table 4 (Agoua and Perré 2010). These data were measured using the same samples as the permeability as shown in Table 1. The diffusion coefficient results for the Australian hardwoods were, in all cases, markedly lower than the published figures. This indicates that the low diffusivity of Australian hardwoods compounds their relatively slow drying rates.

Table 4. Published Longitudinal (L), Radial (R), and Tangential (T) Gas Diffusion Coefficients (D_b) and Anisotropy Ratios for Other Species (Agoua and Perré 2010)

	D_b (m^2 s^{-1})			Anisotropy Ratio		
Species	L×10^{-10}	R×10^{-10}	T×10^{-10}	K_L/K_R	K_L/K_T	K_R/K_T
Maritime pine *(Pinus pinaster)*	143	4.3	2.9	33.1	49.1	1.5
Spruce (*Picea abies*)	196	1.6	1.3	123	148	1.2
Beech (*Fagus sylvatica*)	86	4.8	2.1	18.1	40.6	2.25
Teak (*Tectona grandis*)	40	2.8	1.7	14.1	23.7	1.68

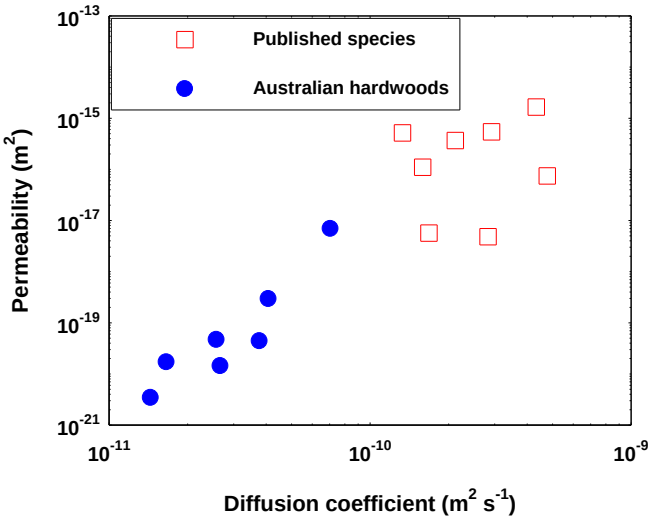

Fig. 9. Relationship between diffusion coefficient and permeability in the radial and tangential directions for Australian hardwoods and published mixed species

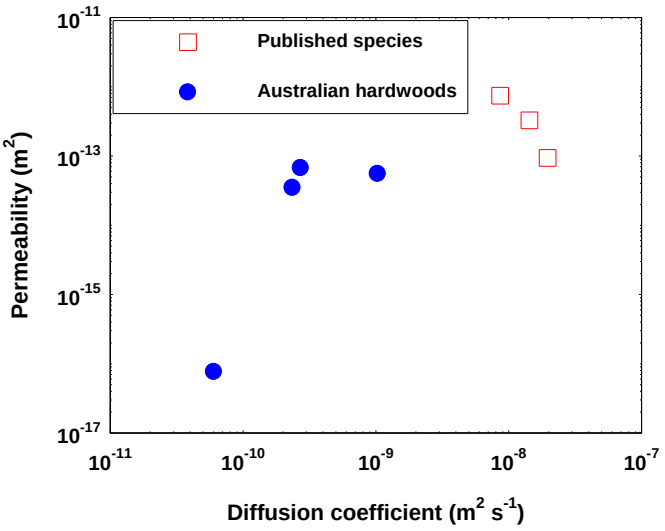

Fig. 10. Relationship between diffusion coefficient and permeability in the longitudinal directions for Australian hardwoods and published mixed species

The relatively low diffusivity and permeability of Australian hardwoods compared to other published hardwood and softwood species can be observed by plotting diffusion coefficients with permeability. This is achieved using the diffusion coefficient and permeability data provided in Tables 1 to 4 as shown in Fig. 8 in the transverse (radial and tangential) directions, and Fig. 9 in the longitudinal direction. It can be observed that in both the transverse and longitudinal directions there is an obvious demarcation between the Australian hardwood and published species groups, emphasizing the slow and difficult nature of removing water from Australian hardwoods.

CONCLUSIONS

1. Characterization of air permeability and diffusivity mass transfer properties were achieved for four highly commercial Australian hardwood species in the longitudinal, radial, and tangential directions.
2. The measurement of previously unpublished, very low wood permeability values through the development of a custom system, based on volume evolution, was achieved.
3. Spotted gum was found to be the most highly impermeable species, particularly in the radial direction as, even after 24 hours, no noticeable measurement could be made.
4. The radial to tangential permeability anisotropy ratio of messmate was in the order of 10^2, markedly higher than for the other species tested.
5. Except for messmate in the radial direction, the four species measured were less permeable in all directions than the lowest published figures, demonstrating the high impermeability of Australian hardwoods partly accounting for their relatively slow drying rates.

6. Diffusion coefficient was lowest in all directions for spotted gum and highest for messmate.
7. The ratio of longitudinal diffusion to both radial and tangential directions is much greater for messmate than spotted gum, indicating messmate's greater propensity for drying in the longitudinal direction. This is advantageous during vacuum drying and acts to complement current vacuum drying modeling research.
8. Comparing the relationship between permeability and diffusion coefficient values of the Australian hardwood species tested and published mixed species in all material orientations reveals markedly lower values for the Australian hardwood species, which highlights their comparatively slow drying rates.
9. The permeability, water-vapour diffusivity, and associated anisotropic ratio data obtained for messmate were extreme or did not follow typical trends compared with other species. Messmate is by far the hardest wood to dry in terms of collapse and checking drying degrades. It seems that heterogeneity and isotropy at this level correlates well with ease of drying.

ACKNOWLEDGMENTS

The substantial contributions of AgroParisTech University - l'École Nationale du Génie Rural des Eaux des Forêts (ENGREF), Queensland University of Technology (QUT), Queensland Cyber Infrastructure Foundation (QCIF), Forest and Wood Products Australia (FWPA), and the Department of Employment, Economic Development and Innovation (DEEDI), to the successful undertaking of this collaborative project are gratefully acknowledged. We would like to thank the anonymous reviewers for their careful reading of the manuscript and for suggesting changes that improved the overall presentation of the work.

REFERENCES CITED

Agoua, E., and Perré, P. (2010). "Mass transfer in wood: Identification of structural parameters from diffusivity and permeability measurements," *Journal of Porous Media* 13(11), 1017-1024.

Agoua, E., Zohoun, S., and Perré, P. (2001). "A double climatic chamber used to measure the diffusion coefficient of water in wood in unsteady-state conditions: Determination of the best fitting method by numerical simulation," *International Journal of Heat and Mass Transfer* 44, 3731-3744.

Bootle, K. R. (2004). *Wood in Australia - Types, Properties and Uses*, McGraw Hill, Sydney.

Dullien, F. A. L. (1992). *Porous Media: Fluid Transport and Pore Structure*, Academic Press Inc., New York.

Moura, M. J., and Figuerido, M. M. (2002). "Characterization of eucalypt wood by mercury porosimetry - Data interpretation," *Bull. Mocrom. Industr. Corp.* 13(5), 8-9.

Pang, S. (2007). "Mathematical modeling of kiln drying of softwood timber: model development, validation and practical application," *Drying Technology* 25, 421-431.

Perré, P. (2007). "Chapter 7 - Fluid migration in wood," *Fundamentals of Wood Drying*, P. Perré (ed.), A.R.BO.LOR, Nancy, 125-156.

Perré, P., and Passard, J. (2004). "A physical and mechanical model able to predict the stress field in wood over a wide range of drying conditions," *Drying Technology* 22, 24-44.

Perré, P., Rémond, R., and Aléon, D. (2007). "Energy saving in industrial wood drying addressed by a multiscale computational model: Board, stack, and kiln," *Drying Technology* 25, 75-84.

Perré, P., and Turner, I. W. (1999a). "A 3-D version of TransPore: A comprehensive heat and mass transfer computational model for simulating the drying of porous media." *Int. J. of Heat and Mass Transfer*, 42, 4501-4521.

Perré, P., and Turner, I. W. (1999b). "Transpore: A generic heat and mass transfer computational model for understanding and visualising the drying of porous media," *Drying Technology* 17(7), 1273-1289.

Redman, A. L. (2011). "Evaluation of super-heated steam vacuum drying viability and development of a predictive drying model for Australian hardwood species," *PR08.2047*, Queensland Government Department of Employment, Economic Development and Innovation report for Forestry and Wood Products Australia. (http://www.fwpa.com.au/Evaluation%20_of_super-heated_steam_vacuum_drying_viability_and_development_of_a_predictive_drying_model, accessed May 18, 2012).

Redman, A. L., Bailleres, H., and Perré, P. (2011). "Characterization of viscoelastic, shrinkage and transverse anatomy properties of four Australian hardwood species," *Wood Material Science & Engineering* 6(3), 95-104.

Rousset, P., Perré, P., and Girard, P. (2004). "Modification of mass transfer properties in poplar wood (*P. robusta*) by a thermal treatment at high temperature," *Holz Roh Werkst*. 62, 113-119.

Salin, J. G. (1991). "Modeling of wood drying: A bibliography," *Drying Technology* 9, 775-793.

Salin, J. G. (2010). "Problems and solutions in wood drying modelling: History and future," *Wood Material Science and Engineering* 5, 123-134.

Savard, M., Lavoie, V., and Trembala, C. "Technical and economical assessment of superheated steam vacuum drying of northern red oak." *N.A.G.R.E.F. COST E15 Conference*, Athens, Greece, 1-10.

Siau, J. F. (1984). *Transport Processes in Wood*, Springer-Verlag, Germany.

Turner, J. W., and Perré, P. (1995). "A comparison of the drying simulation codes TransPore amd Wood2D which are used for the modelling of two-dimensional wood drying processes," *Drying Technology, Special issue: Mathematical Modeling and Numerical Techniques for the Solution of Drying Problems* 13(3), 695-735.

Vermaas, H. F. (1995). "Drying eucalypts for quality: Material characteristics, pre-drying treatments, drying methods, schedules and optimisation of drying quality," *South African Forestry Journal* 174, 41-49.

Vermaas, H. F., and Bariska, M. (1995). "Collapse during low temperature drying of *Eucalyptus grandis* W. Hill and *Pinus silvestris* L." *Holzforchung*, 2, 35-40.

Article submitted: February 14, 2012; Peer review completed: April 22, 2012; Revised version received: June 3, 2012; Accepted: June 8, 2012; Published: June 18, 2012.